EPJ Web of Conferences **227**, 02010 (2020) https://doi.org/10.1051/epjconf/202022702010
10th European Summer School on Experimental Nuclear Astrophysics

Elastic Scattering and Reaction Cross-section of ^{8}Li on ^{209}Bi

C. Sengupta[1,*], *K.J.* Cook[2], *E.C.* Simpson[1], *M.* Dasgupta[1], *D.J.* Hinde[1], *K.* Banerjee[3], *L.T.* Bezzina[1], and *M.A.* Stoyer[4]

[1]Department of Nuclear Physics, Research School of Physics, The Australian National University, Canberra, Australian Capital Territory 2601, Australia
[2]Department of Physics, Tokyo Institute of Technology, 2-12-1 O-Okayama, Meguro, Tokyo 152-8551, Japan
[3]Variable Energy Cyclotron Centre, 1/AF, Bidhan Nagar, Kolkata 700064, India
[4]Nuclear and Chemical Sciences Division, Lawrence Livermore National Laboratory, Livermore, CA 94550 USA

Abstract. Nuclear physics in the 21st century is driven by a quest to understand the properties of ever more exotic nuclear systems. Unusual structural phenomena are observed to arise in light weakly bound nuclei such as ^{8}Li. ^{8}Li has a cluster structure core of ^{7}Li surrounded by a loosely bound neutron which is observed to influence reaction mechanisms near the fusion barrier. Elastic scattering provides a vital step towards understanding more complicated reaction mechanisms. In this work, elastic scattering was measured for ^{8}Li + ^{209}Bi at energies 2% to 34% above the barrier, allowing extraction of reaction cross-sections. The systematics of the reaction cross-sections of ^{8}Li compared to neighbouring nuclei ^{6,7,9,11}Li are discussed.

1 Introduction

Experimental and technological advances in the last few decades have allowed us to explore the structure and properties of nuclei from stability up to and beyond the driplines, where nuclides become unbound. The lithium isotopes are particularly interesting as they exhibit a range of structural properties that may influence nuclear reaction mechanisms. The relatively well-bound ^{6,7}Li show cluster structures, which means they can be easily broken into an α and a ^{2,3}H respectively. Reaction cross-sections obtained for ^{6,7}Li + ^{208}Pb from precise elastic scattering data measured by Keeley *et al.* [1] at energies above the barrier were found to be similar, with a slightly larger reaction cross-section for ^{6}Li attributed to a smaller breakup threshold (1.473 MeV) compared to that of ^{7}Li (2.467 MeV). On the other end of this isotopic chain, is the exotic nucleus ^{11}Li, which has two loosely bound neutrons (S_{2n} = 0.369 MeV) around a relatively well-bound ^{9}Li core. This results in a long tail in its density distribution and gives rise to very large reaction cross-sections at energies below and above its expected barrier [2, 3]. ^{8}Li is intermediate between ^{7}Li and ^{11}Li and can be thought to consist of a cluster structure core of ^{7}Li and a loosely bound neutron (S_{n} = 2.03 MeV). To understand the

*e-mail: Chandrima.Sengupta@anu.edu.au

effect of this intermediate structure of ^{8}Li on reaction cross-sections, precise elastic scattering measurements are necessary.

To achieve this, elastic scattering angular distributions were measured for the reaction ^{8}Li + ^{209}Bi at energies 2% - 11% above the barrier. Elastic scattering data were also measured for this system at energies 25% - 34% above the barrier and reported in Ref. [4]. Combining these data allows us to perform a thorough optical model analysis to obtain reaction cross-sections and provide a consistent description of elastic scattering. The systematics of reaction cross-sections for ^{8}Li will then be compared with ^{6,7,9,11}Li data from the literature. The reaction cross-sections obtained for ^{8}Li will as well as be compared with the results obtained from high energy cross-section measurements, where similar root mean square (rms) nuclear radii were found for ^{6,7,8,9}Li [5].

2 Experimental Setup

The elastic scattering measurements were performed using the SOLEROO (SOLenoidal Exotic Rare isOtOpe separator) radioactive ion beam (RIB) capability [6, 7] at the Australian National University (ANU). This is based on a 6.5 T super-conducting solenoidal separator and produces RIBs by the in-flight transfer method [8]. The trajectories of the RIBs are tracked with two position sensitive parallel plate avalanche counters (PPACs) [9]. The elastically scattered particles from the secondary target were measured with an array consists of four double-sided silicon strip detectors (DSSDs) (Breakup Array for Light Nuclei, BALiN), each 400 μm thick. Each DSSD in the BALiN array has 16 arcs in θ and 8 sectors in ϕ, giving a total 512 pixels. Position, energy and Time of Fight (ToF) information can be obtained for each pixel of the BALiN array. BALiN was placed in the front-back configuration surrounding the secondary target providing an angular coverage from 25° - 155° in θ, with a constant total ϕ coverage of 135° over this angular range.

The ^{7}Li primary beam was delivered by the ANU Heavy Ion Accelerator Facility [10, 11] and bombarded a 5.57 mg/cm^2 ^{9}Be target. The primary ^{7}Li beams of 36 MeV and 39.2 MeV were pulsed, with 0.8 ns full width at half maximum (FWHM) bunches being delivered every 107 ns by the accelerator so that the ToF information could be obtained with respect to the RF signal. The ^{8}Li secondary beam was produced in a single neutron transfer in the production reaction ^{7}Li (^{9}Be, ^{8}Li) ^{8}Be with the differential cross-section of the reaction being 30 mb/sr [8]. Following production, the ^{8}Li beam is brought to a focus on a ^{209}Bi secondary target with the super-conducting solenoidal separator, which has an acceptance between 2° and 6°. The direct ^{7}Li primary beam is stopped by a Faraday cup in front of the entrance of the solenoid. Some of the contaminants in the secondary beam are focussed on an axial rod and blocked by the blocking discs placed along the axial rod.

In the production reaction, ^{8}Li can be populated in the ground state in the reaction ^{7}Li + ^{9}Be $\rightarrow$ ^{8}Li$_{GS}$ + ^{8}Be$_{GS}$ (82%), in its first excited state ^{7}Li + ^{9}Be $\rightarrow$ ^{8}Li (0.98 MeV state [12]) + ^{8}Be$_{GS}$ (17%), and, ^{8}Be in its resonance state at 3.03 MeV in the reaction ^{7}Li + ^{9}Be $\rightarrow$ ^{8}Li$_{GS}$ + ^{8}Be (3.03 MeV state) (1%). The bracketed percentages give the fraction of the total ^{8}Li flux transmitted to secondary target. The proportions of each of these groups were measured by employing a Si ΔE - E detector which was swung in at the secondary target position before performing the elastic scattering measurement. The 0.98 MeV excited state of ^{8}Li decays to ^{8}Li$_{GS}$ by emitting a 980 keV γ ray [12] before reaching the secondary target. Taking into account the energy losses of these three energy groups in the primary target, and in the PPACs as well as the Q value of ^{8}Li transfer reaction, the mean ^{8}Li energies at the mid point of the 1.25 mg/cm^2 ^{209}Bi target at 45° to the beam axis were 31.4 MeV and 34.1 MeV for the ^{7}Li primary beam energies of 36 MeV and 39.2 MeV respectively.

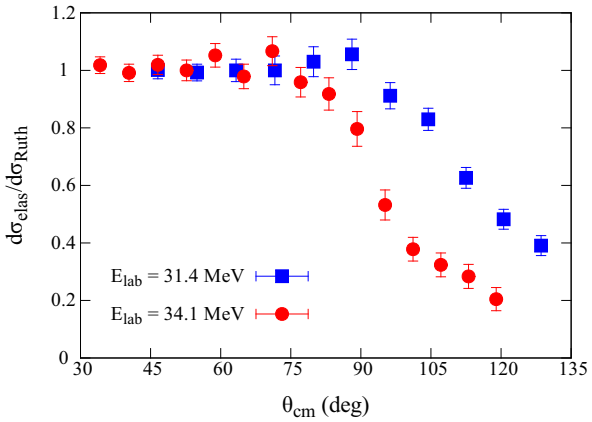

Figure 1: $\frac{d\sigma_{elas}}{d\sigma_{Ruth}}$ as a function of θ_{cm} for ^{8}Li at E_{lab} = 31.4 MeV and 34.1 MeV. The quoted energies are the mean ^{8}Li energies at the centre of the ^{209}Bi target. These results are preliminary.

3 Elastic Scattering Angular Distribution

As a result of solenoid angular acceptance of 2° to 6°, the angle of incidence of the ^{8}Li beam on the secondary target ranges between ±6°. The secondary beam also has a finite size (FWHM ~ 9 mm) on the secondary target. Both these factors can change the scattering angle. Elastic scattering cross-sections, being proportional to $\frac{1}{\sin^4(\theta/2)}$, demand the reconstruction of the true scattering angle which entails the development of reconstruction routines to track the RIB trajectory.

Every particle incident on the secondary target is tracked with the two PPACs. The position information obtained from the two PPACs have been utilised to reconstruct the secondary target interaction point and angle of incidence of the ^{8}Li beam on the secondary target on an event-by-event basis. These have been used to obtain the true scattering angle, θ_{RIB} of every elastically scattered event.

Once the true scattering angles are calculated, the elastic events are identified from experimental data consistently at all angles. The elastic yield obtained at each energy is then normalised to Rutherford scattering using a Monte Carlo simulation which incorporates the RIB size and offset. A sub-barrier measurement was also performed for ^{8}Li on ^{208}Pb at 15.4 MeV and was used for overall solid angle normalisation for all the above barrier measurements since at this energy elastic scattering should strictly follow Rutherford scattering at all angles. Preliminary results for the elastic scattering angular distributions are shown in Fig. 1.

4 Reaction Cross-section

Reaction cross-sections were obtained from the elastic scattering angular distributions (shown in Fig. 1 and from Ref. [4]) for ^{8}Li + ^{209}Bi using an optical model analysis [13] using FRESCO, version frxy [14].

In this analysis, a volume Woods-Saxon form [15] has been used as an interaction potential between the target and the projectile. In order to obtain a good fit to the measured data of ^{8}Li + ^{209}Bi, some reasonable constraints are imposed on the optical model parameters. We

Table 1: Summary of the reaction cross-sections for ^{8}Li + ^{209}Bi. The parameters of the real Woods-Saxon potential were fixed at V_0 = 113 MeV, r_0 = 1.122 fm and a = 0.63 fm during the fitting procedure which reproduce the average fusion barrier 29.39 MeV in the centre-of-mass frame.

E_{lab} (MeV)	$\sigma_{reaction}$ (mb)	$\Delta\sigma^{stat}$ (mb)	$\Delta\sigma^{stat}$ (%)
40.9	1435.0	12	0.8%
39.9	1346.0	14	1.0%
38.2	1287.0	20	1.6%
34.1	697.8	30	4.4%
31.4	396.3	23	6.1%

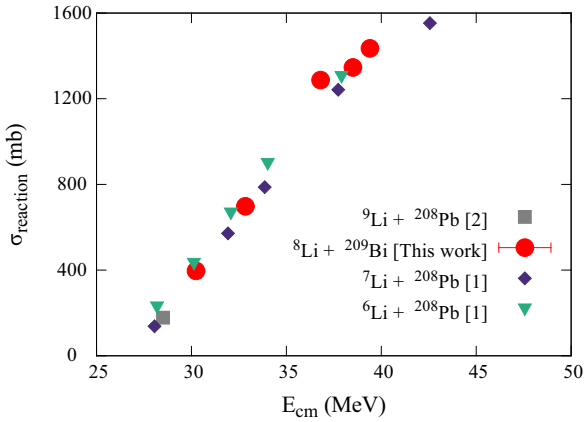

Figure 2: Reaction cross-sections and the corresponding statistical uncertainties as a function of E_{cm} for ^{6,7}Li on ^{208}Pb (Keeley *et al.* [1]), ^{8}Li on ^{209}Bi (present data), and ^{9}Li on ^{208}Pb (Cubero *et al.*, [2]). Present results are preliminary.

fixed the real parameters V_0 = 113 MeV, r_0 =1.122 fm and a = 0.63 fm of the phenomenological Woods-Saxon potential to be such that the parameters reproduce the expected fusion barrier of ^{8}Li + ^{209}Bi (29.39 MeV) extrapolated from ^{6,7}Li barriers from Ref. [16]. The barrier energies obtained by scaling is expected to be reasonable as ^{8}Li has only one extra neutron and its matter radius is very close to that of ^{6,7}Li [5]. To obtain an initial guess for the imaginary Woods-Saxon parameters W_0, r_w and a_w, a 3 D χ^2/N surface is generated to find the minimum χ^2/N that represents the best fit to the experimental data, N being the number of degrees of freedom. The minima of the χ^2/N surfaces corresponding to W_0, r_w and a_w have then been used as an initial guess in FRESCO to fit the data. The reaction cross-sections obtained from these fits are given in Table 1. The data do not allow us to provide unique optical model parameters and hence the fitted parameters are not given here. The corresponding statistical uncertainties, $\Delta\sigma^{stat}$ are also given in Table 1. Preliminary results obtained in this work were then compared with neighbouring lithium isotopes ^{6,7,9}Li available in the literature, shown in Fig. 2 as a function of centre-of-mass energy.

It can be seen from Fig. 2, the reaction cross-sections obtained for ^{8}Li are very similar to those of ^{6,7,9}Li from Ref. [1] and [2], respectively. Reaction cross-sections for light ions are in general sensitive to the binding energy of the least well-bound nucleons, and hence to the lowest breakup threshold. The lowest breakup thresholds for ^{6}Li, ^{7}Li, ^{8}Li, ^{9}Li and ^{11}Li are respectively, 1.5 MeV, 2.5 MeV, 2.03 MeV, 4.1 MeV and 0.369 MeV. Comparing these values, ^{6}Li, ^{7}Li, ^{8}Li and ^{9}Li have similar lowest breakup thresholds. Hence, to first order, similar reaction cross-sections might be expected for ^{6}Li, ^{7}Li, ^{8}Li and ^{9}Li, as seen in Fig. 2. ^{11}Li has a very small breakup threshold correlated with a very large reaction cross-sections (5400 mb at E_{lab} = 24.3 MeV and 7800 mb at E_{lab} = 29.8 MeV [2, 3]) compared to ^{6,7,8,9}Li.

5 Conclusions

We have measured elastic scattering for ^{8}Li + ^{209}Bi. We conclude that no significant difference is observed in the lithium isotopes in terms of reaction cross-sections except for ^{11}Li, which has unique structure. The deduced reaction cross-sections are consistent with the trend of the rms nuclear radii of the lithium isotopes determined from high energy reaction cross-section measurements in Ref. [5].

This work was supported by the Australian Research Council Grants No. DP170102423, No. DP160101254, No. DP170102318, and No. DP190101442. Support for ANU Heavy Ion Accelerator Facility operations through the NCRIS program is acknowledged. The work was partially performed under the auspices of the U.S. Department of Energy by Lawrence Livermore National Laboratory under contract DE-AC52-07NA27344.

References

[1] N. Keeley *et al.*, Nuc. Phys. A **571**, 326-336 (1994).
[2] M. Cubero *et al.*, Phys. Rev. Lett. **109**, 262701 (2012).
[3] J. P. Fernandez-Garcia *et al.*, Phys. Rev. C **92**, 044608 (2015).
[4] K. J. Cook *et al.*, Phys. Rev. C **97**, 021601(R) (2018).
[5] I. Tanihata *et al.*, Phys. Rev. Lett **55**, No. 24, 2676-2679 (1985).
[6] R. Rafiei *et al.*, Nuc. Instr. and Meth. in Phys. Res. A **631**, 12-21 (2011).
[7] I. P. Carter *et al.*, EPJ Web of Conf. **91**, 00001 (2015).
[8] A.J. Horsley *et al.*, Nuc. Instr. and Meth. in Physics Res. A **646**, 174–183 (2011).
[9] Ian P. Carter, "Developing techniques for high fidelity studies of reactions with light weakly bound nuclei", Ph.D. Thesis, The Australian National University (2016).
[10] T. R. Ophel *et al.*, Nuc. Instr. and Meth. **122**, 227 - 234 (1974).
[11] A. E. Stuchbery *et al.*, Nuc. Instr. and Meth. in Phys. Res. A **382**, 172-175 (1996).
[12] D. R. Tilley *et al.*, Nuc. Phys. A **745**, 155-362 (2004).
[13] H. Feshbach *et al.*, Phys. Rev. **96**, No. 2, 448-464 (1954).
[14] I. J. Thompson, Compt. Phys. Rep. **7**, 167-212 (1988).
[15] Roger D. Woods *et al.*, Phys. Rev. **95**, 577-578 (1954).
[16] M. Dasgupta *et al.*, Phys. Rev. C **70**, 024606 (2004).